

Coherent backscattering spectroscopy

Young L. Kim, Yang Liu, Vladimir M. Turzhitsky, Hemant K. Roy, Ramesh K. Wali, and Vadim Backman

Department of Biomedical Engineering, Department of Gastroenterology, Northwestern University, Evanston, Illinois 60208

Received February 18, 2004

Coherent backscattering (CBS) of light in random media has been previously investigated by use of coherent light sources. Here we report a novel method of CBS measurement that combines low spatial coherence, broadband illumination, and spectrally resolved detection. We show that low spatial coherence illumination leads to an anomalously broad CBS peak and a dramatic speckle reduction; the latter is further facilitated by low temporal coherence detection. Thus CBS can be observed in biological tissue and other media that previously were beyond the reach of conventional CBS measurements. We also demonstrate, for the first time to our knowledge, spectroscopic analysis of CBS. CBS spectroscopy may find important applications in probing random media such as biological tissue in which depth-selective measurements are crucial. © 2004 Optical Society of America

OCIS codes: 030.1670, 290.1350, 300.6170, 170.4580.

Coherent backscattering (CBS) of light by random media is a phenomenon in which waves traveling time-reversed paths interfere constructively, thus generating a peak of scattered light intensity in the backward direction.^{1–4} Conventionally, in diffusion approximation the CBS peak is determined mainly by the transport mean free path length l_s^* and has a full angular width at half-maximum of

$$w \approx \lambda / (3\pi l_s^*), \quad (1)$$

where λ is the wavelength of light.¹ Although the phenomenon of CBS has recently attracted significant interest and has been an object of intensive investigation in nonbiological media,^{1,2} there have been only a few reports of CBS observation in biological tissues.^{3,4} The application of CBS for tissue characterization has been hampered by several factors: (1) The angular width of CBS is inversely proportional to l_s^* . In tissue, $l_s^* \approx 500\text{--}2000 \mu\text{m}$ and $w \approx 0.001^\circ$. Experimental observation of such extremely narrow peaks is difficult, in part because the CBS signal can be masked by speckle.⁴ (2) CBS measurements have relied on coherent single-wavelength laser light sources, which do not permit measurement of the spectral properties of CBS. (3) Because most biological tissues have multilayered structure, depth-selective measurements are crucial.^{5,6} However, depth-selective CBS measurements currently require expensive femtosecond illumination and detection³ that also prevent collection of spectral information.

In this Letter we show, for the first time to our knowledge, that one can achieve path-length selectivity, speckle reduction, and spectroscopic information by combining CBS measurements with (1) low spatial coherence (LSC) illumination, (2) low temporal coherence detection, and (3) broadband illumination and spectrally resolved detection, i.e., low-coherence backscattering (LCBS). We developed a novel LCBS instrument that facilitates simultaneous measurement of the spectral (400–700-nm) and the scattering-angle (-5° to 5° in the backward direction) properties of light

scattering [Fig. 1(a)]. A beam of broadband cw light from a 500-W Xe lamp (Oriel) was collimated by a 4- f lens system L1–A1–L2 (divergence, $\theta = 0.03^\circ\text{--}0.10^\circ$), polarized, and delivered onto a sample at a 15° angle of incidence to prevent the collection of specular reflection. The spatial coherence length of illumination L_{SC} was varied from 110 to $180 \mu\text{m}$ by means of aperture A1 and confirmed by double-slit interference. The light backscattered by a sample was collected by a Fourier lens, a polarizer oriented along the polarization of the incident light, and an imaging spectrograph (Acton Research). The spectrograph was positioned in the focal plane of the Fourier lens and coupled to a CCD camera (CoolSnapHQ, Roper Scientific). As shown in Fig. 1(b), the Fourier lens projected the angular distribution of the backscattered light onto the slit of the spectrograph. Then the spectrograph dispersed this light according to its wavelength in the direction perpendicular to the slit. Thus the CCD recorded a matrix of light-scattering intensities as a function of wavelength λ and backscattering angle θ . The temporal coherence length of detection was determined by the spectral resolution of the spectrograph, $L_{TC} = [(2 \ln 2) / \pi]^{1/2} (\lambda^2 / \Delta\lambda) = 30 \mu\text{m}$, where $\Delta\lambda = 9 \text{ nm}$ is the FWHM of the detection bandpass. The CBS peaks were normalized by the incoherent baseline scattering intensity measured at large

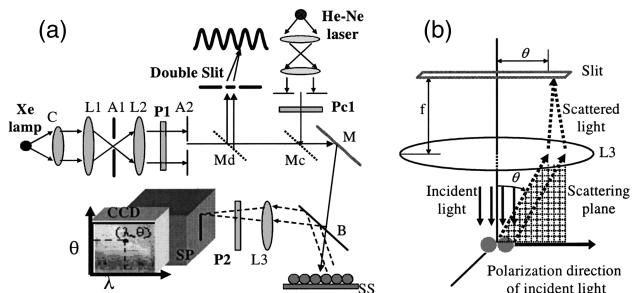


Fig. 1. LCBS spectroscopy instrument. (a) Condenser; L1–L3, lenses; A1, A2, apertures; P's, polarizers; M's, mirrors; B, beam splitter; SS, sample stage; SP, spectrograph. (b) Unfolded view of light trajectories without the beam splitter.

backscattering angles ($\theta > 1^\circ$). To compensate for the finite point-spread function of the detection system and the incident beam divergence, we deconvolved the profiles of the CBS peaks with the angular response of the instrument. To compare our measurements with the conventional CBS theory, which assumes coherence illumination, we also used a He–Ne laser (Melles Griot).

Figure 2(a) shows the angular distribution of a typical backscattering signal collected from *ex vivo* rat colon tissue under LSC illumination ($L_{SC} = 140 \mu\text{m}$, i.e., $L_{SC} \ll l_s^*$, and $\lambda = 632 \text{ nm}$). A CBS peak can be clearly identified. As discussed below, this low-coherence CBS possesses novel and intriguing properties: lack of speckle, dramatic broadening of the CBS peak, and ability to be studied as a function of wavelength (i.e., CBS spectroscopy). Indeed, for comparison, Fig. 2(b) shows the angular distribution of the backscattered light obtained from the same tissue site when a coherent He–Ne laser was used. Evidently, in the case of spatially and temporally coherent illumination [Fig. 2(b)] the speckle masks the profile of a CBS peak in the absence of Brownian motion of the scattering particles, in dramatic contrast with the speckle-free ICBS peak of Fig. 2(a). Furthermore, Fig. 2(c) shows a CBS peak simulated by use of the conventional diffusion-approximation theory¹ of CBS for $l_s^* = 660 \mu\text{m}$. Evidently, the conventional CBS peak is much narrower, with $w \approx 0.001^\circ$. The angular width of the CBS peak observed under LSC illumination [Fig. 2(a)] is 0.3° , more than 100 times greater than the width of the peak predicted by the conventional theory [expression (1)].

First, we discuss the origins of the dramatic and *a priori* surprising ICBS broadening. We hypothesize that ICBS broadening is due primarily to LSC illumination, i.e., that $L_{SC} \ll l_s^*$. Under spatially coherent illumination ($L_{SC} > l_s^*$), any conjugated time-reversed waves can interfere with one another constructively, thus giving rise to the CBS effect. For LSC illumination, however, only the light paths with the first and the last points within the area of coherence can interfere constructively. As a result, LSC illumination prevents long light paths from contributing to CBS. The width of a CBS peak is directly related to the origin of the CBS signal: Longer light paths correspond to small scattering angles, whereas short paths give rise to CBS at larger angles.¹ Thus, under LSC illumination, the width of CBS is increased because it is generated predominantly by photons traveling short paths. We investigated the effect of LSC illumination on CBS by using physical tissue models consisting of aqueous suspensions of polystyrene microspheres (Duke Scientific) of various diameters from 200 to 980 nm. We studied the CBS profiles by varying l_s^* from 20 to 1000 μm ($L_{SC} = 140 \mu\text{m}$). As shown in Fig. 3(a), for spatial coherence illumination the inverse CBS peak width w^{-1} increases linearly with l_s^* , in agreement with the prediction of the conventional CBS theory and expression (1). For comparison, the dependence of w^{-1} on l_s^* for LSC illumination is remarkably different. As shown in Fig. 3(b), for $l_s^* < L_{SC}$ (Regime A), w^{-1} increases

with l_s^* , as expected. However, for $l_s^* \geq L_{SC}$, w^{-1} first decreases with l_s^* (Regime B) and then reaches a plateau independently of l_s^* for $l_s^* \gg L_{SC}$ (Regime C). For LSC illumination the CBS peak is substantially broadened, which agrees with the CBS data measured from the tissue [Fig. 2(a)]. Thus we can conclude that, for $l_s^* \gg L_{SC}$, the CBS peak width is not determined by l_s^* . We then studied the dependence of CBS on L_{SC} . Figure 3(c) shows w^{-1} measured for L_{SC} ranging from 110 to 180 μm with $l_s^* = 2 \text{ mm}$ at $\lambda = 632 \text{ nm}$. Evidently, the CBS peaks become narrower as L_{SC} increases, because a larger L_{SC} allows longer light paths to contribute to CBS. Thus, in the LSC regime, w is determined primarily by L_{SC} , $w \propto \lambda/L_{SC}$. We conclude that LSC illumination broadens CBS peaks, thus facilitating depth-resolved CBS measurements in tissue.

The second crucial feature of ICBS is dramatic speckle reduction. Speckle has been one of the limiting factors hampering CBS study in biological tissue.⁴ Each area of spatial coherence generates its unique speckle pattern. If $L_{SC} \ll D$, where D is the size of the illumination or collection area, $\sim (D/L_{SC})^2 \sim 100$ independent speckle spots are simultaneously sampled.

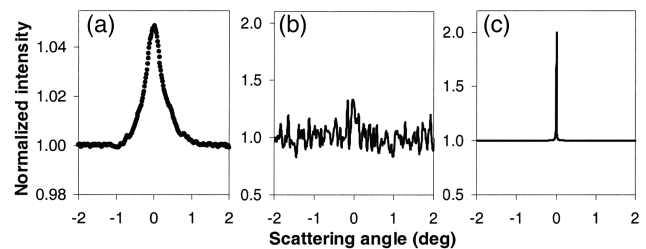


Fig. 2. Normalized angular distributions of backscattering from rat colon tissue. (a) Experimental data, LSC illumination (Xe lamp). (b) Experimental data, coherent illumination (He–Ne laser). (c) Simulation from the conventional diffusion-approximation-based CBS theory¹ for $l_s^* = 660 \mu\text{m}$.

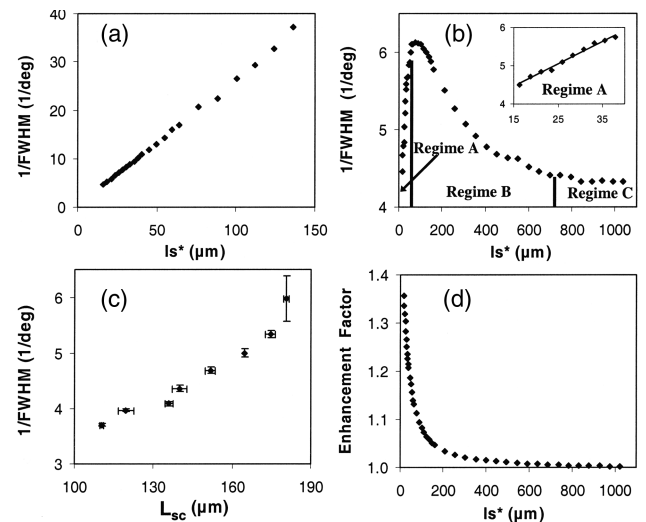


Fig. 3. Inverse CBS peak width w^{-1} as a function of l_s^* for (a) coherent illumination (He–Ne laser) and (b) LSC illumination (Xe lamp). (c) w^{-1} as a function of L_{SC} ($l_s^* = 2 \text{ mm}$). (d) CBS enhancement factor for LSC illumination.

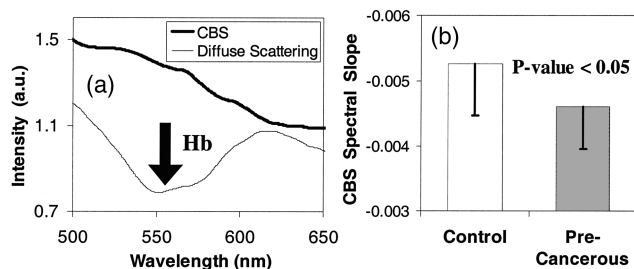


Fig. 4. ICBS spectroscopy of rat colon tissues for detection of early precancer. (a) Normalized diffuse intensity measured from the colon of a rat treated with azoxymethane (AOM) and CBS spectrum measured from the same site. (b) Slopes of the CBS spectra ($\lambda = 520\text{--}650\text{ nm}$) obtained from precancerous and control tissues.

Low temporal coherence detection ($L_{TC} \ll L_{SC}$) further increases this number by $\sim(L/L_{TC}) \sim 10$, where L is the average path length. Thus ICBS averages over ~ 1000 independent speckle patterns, which results in speckle suppression and in the possibility of observing speckle-free CBS.

Finally, broadband illumination and spectroscopic detection embedded in the ICBS instrument open the possibility of studying CBS as a function of wavelength. We found that for LSC illumination the CBS enhancement factor decreases with l_s^* [Fig. 3(d)]. Thus, because l_s^* varies with wavelength in biological tissue, the wavelength dependence of $l_s^*(\lambda)$ can be assessed from the CBS spectra. As discussed below, spectroscopic information is of crucial importance for tissue diagnosis. Evidently, such information could not previously be obtained in conventional single-wavelength CBS measurements.

Elastic light scattering has been shown to be extremely sensitive to morphological and biochemical alterations in tissues.^{5,7} Because the most superficial tissue layer, the epithelium, which can be as thin as $20\text{--}30\ \mu\text{m}$, is the origin of nearly 90% of human cancers, considerable effort has been expended to develop optical techniques to target this thin layer selectively.⁵ Light absorption in the blood vessels located below the epithelium presents an additional problem, as hemoglobin absorption spectra obscure the endogenous spectral signatures of epithelial cells. This difficulty can be avoided by use of depth-selective ICBS spectroscopy.

To demonstrate the potential benefits of ICBS spectroscopy for precancer diagnosis, we conducted studies involving an experimental model of colon cancer: Fisher-344 rats treated with a colon-specific carcinogen, AOM ($n = 92$). The AOM-treated rat model is one of the most robust and widely used animal models of colon cancer.⁸ In this model the earliest detectable markers of carcinogenesis, aberrant crypt foci, develop in 5–10 weeks after the AOM injection, and adenomas are observed in 20–30 weeks. The rats were divided into two equal groups. One group was injected twice weekly with a dose of AOM (15 mg/kg of body

weight), and the other group received an injection of saline twice weekly. After 2 weeks of AOM or saline injections, the rat colons were excised. At this early stage of carcinogenesis, the disease cannot be diagnosed by any currently available histological or molecular method.

Figure 4(a) shows a typical spectrum (thin, solid curve) of diffusely reflected light from a rat's colonic mucosa. This signal exhibits a characteristic hemoglobin absorption band near 550 nm. For comparison, Fig. 4(a) also shows the spectrum of a CBS signal (thicker curve) recorded with $L_{SC} = 140\ \mu\text{m}$ from the same tissue sample and integrated over a scattering angle within the CBS peak. The CBS spectrum in Fig. 4(a) does not exhibit any hemoglobin absorption bands, thus supporting the conclusion that the CBS peaks arise from photons localized within the epithelium.

We identified significant differences between the CBS spectra recorded from the control and the precancerous tissues. Specifically, the change in the linear slopes of the CBS spectra in the wavelength range $\lambda = 520\text{--}650\text{ nm}$ was found to be highly significant between the two groups [P value < 0.05 ; Fig. 4(b)]. These changes in the CBS spectra indicate that the precancerous epithelial cells develop distinct optical properties very early in carcinogenesis. This fact can be exploited to identify previously undetectable precancerous lesions far earlier than with currently available histological or molecular diagnoses. In conclusion, we have reported the development of ICBS spectroscopy and have shown that low coherence effects permit CBS measurements to be made in biological tissue and other media with long transport mean free paths.

This study was supported in part by National Science Foundation grant BES-0238903. We thank A. Taflove for helpful discussions and the anonymous reviewers for their comments. Y. L. Kim's e-mail address is younglae@northwestern.edu.

References

1. M. B. van der Mark, M. P. van Albada, and A. Lagendijk, *Phys. Rev. B* **37**, 3575 (1988).
2. A. Wax, S. Bali, and J. E. Thomas, *Phys. Rev. Lett.* **85**, 66 (2000).
3. K. M. Yoo, F. Liu, and R. R. Alfano, *J. Opt. Soc. Am. B* **7**, 1685 (1990).
4. G. Yoon, D. N. G. Roy, and R. C. Straight, *Appl. Opt.* **32**, 580 (1993).
5. Y. L. Kim, Y. Liu, R. K. Wali, H. K. Roy, M. J. Goldberg, A. K. Kromin, K. Chen, and V. Backman, *IEEE J. Sel. Top. Quantum Electron.* **9**, 243 (2003).
6. S. L. Jacques, J. C. Ramella-Roman, and K. Lee, *J. Biomed. Opt.* **7**, 329 (2002).
7. K. Sokolov, M. Follen, and R. Richards-Kortum, *Curr. Opin. Chem. Biol.* **6**, 651 (2002).
8. M. Kobaek-Larsen, I. Thorup, A. Diederichsen, C. Fenger, and M. R. Hoitinga, *Comp. Med.* **50**, 16 (2000).